

Available online at www.sciencedirect.com

ScienceDirect

Procedia CIRP 94 (2020) 850–855

www.elsevier.com/locate/procedia

11th CIRP Conference on Photonic Technologies [LANE 2020] on September 7-10, 2020

Milling applications with GHz burst: Investigations concerning the removal rate and machining quality

Stefan M. Remund^{a*}, Markus Gafner^a, Michalina V. Chaja^a,
Aivaras Urniezius^b, Simas Butkus^b, Beat Neuenschwander^a

^aBern University of Applied Sciences, Institute for Applied Laser, Photonics and Surface technologies, Pstalostrasse 20, 3400 Burgdorf, Switzerland

^bLIGHT CONVERSION, Keramiky Street 2B, Vilnius, LT-10233, Lithuania

* Corresponding author. Tel.: +41-34-426-4221; fax: +41-34-426-1513. E-mail address: stefan.remund@bfh.ch

Abstract

GHz-bursts were reported to be highly efficient for ultra-short pulse laser ablation compared to single pulses. However, most comparisons were made for a drilling process or the machining of dimples. We investigated GHz-bursts (5.4 GHz) on copper, brass, stainless steel, silicon, zirconium oxide, soda-lime glass and sapphire for surface structuring applications. Inconsistent with the published results neither a higher removal rate, nor an improvement in the machining quality in case of the metals and silicon was observed, in the contrary, a tremendous drop in the specific removal rate of 90% for the metals and 60% for silicon, compared to single pulses, was measured when a 25 pulse burst (maximum of laser system) was applied. The situation differs for zirconium oxide, where only a moderate influence was observed and for soda-lime glass and sapphire where the specific removal rate increased by a factor of 2.3 and 6, when the number of pulses per burst were raised from 1 to 25.

© 2020 The Authors. Published by Elsevier B.V.

This is an open access article under the CC BY-NC-ND license (<http://creativecommons.org/licenses/by-nc-nd/4.0/>)

Peer-review under responsibility of the Bayerisches Laserzentrum GmbH

Keywords: Laser microprocessing, ultra short pulses, GHz bursts, laser matter interaction, ablation efficiency, optimum fluence

1. Introduction

High throughput surface structuring with ultra-short laser pulses is still a demanding task. Especially metals, but also many other materials, show an optimum point where most volume per energy can be removed i.e. the specific removal rate shows a maximum value [1-3] going with an optimum peak fluence of e^2 times the threshold fluence in case of a Gaussian beam. Working at this optimum point also guarantees a high surface and machining quality, especially in case of steels, often used for industrial applications. For spot radii in the range of 10 μm – 25 μm , often used for micromachining applications, this leads to corresponding pulse energies of some tens of μJ and therefore, to very high repetition rates, up into the range of several tens of MHz for high average powers [3,4]. With an average power of 187 W, 10 ps pulse duration and using polygon line scanners removal rates up to 27.8 mm^3/min ,

21.4 mm^3/min , 15.3 mm^3/min and 129.1 mm^3/min were achieved for aluminum, copper, stainless steel and Al_2O_3 [5] respectively. But this scale-up process is limited by particle/plasma shielding [4,6] and/or heat accumulation [7] as also shown in [4], where removal rates for steel and copper up to 35.4 mm^3/min respectively 39.5 mm^3/min have been achieved with about 300W of average power and a pulse duration of 3 ps.

However, standard galvo-scanners offer much higher flexibility and are therefore often preferred for micromachining applications. Due to their limited marking speeds, solutions enabling high average power at moderate repetition rates are highly demanded. Pulse bursts (with 10 ns – 30 ns intra burst time intervals) offer such a solution and reduce the requirements for a very high repetition rate and marking speed. First publications in case of ultra-short pulses denoted the bursts to be more efficient compared to single pulses [8] but the

reported benefit was often only due to the reduced peak fluence of a single pulse in the burst [9]. A closer look reveals a more complex behavior. For surface texturing applications, some metals, e.g. copper, show a strongly reduced specific removal rate for even numbers of pulses per burst, whereas its values increases for uneven numbers [10,11]. This behavior seems to be affected by shielding effects and an increase absorptivity of the machined surface [12,13].

Recently GHz-bursts with very short intra burst time intervals have attracted a lot of attention. A first publication with 300 fs pulses at a wavelength of 1030 nm reported specific removal rates up to approximately $7.6 \mu\text{m}^3/\mu\text{J}$ for copper and $13 \mu\text{m}^3/\mu\text{J}$ for silicon [14]. These values could even be increased to $42.2 \mu\text{m}^3/\mu\text{J}$ for silicon [15] and $11.5 \mu\text{m}^3/\mu\text{J}$ for copper [16]. A so called “ablation cooling” effect was supposed to be responsible for these high specific removal rates. However, these results were obtained for punching applications like drilling or machining of dimples. These processes can strongly profit from heat accumulation combined with melt ejection. For instance, the latent heat of fusion amounts 13.3 kJ/mol and the one of vaporization 305 kJ/mol for copper, i.e. a process basing only on the melt phase would be a factor of 23 more efficient as a process demanding full vaporization. Experiments and simulations reported that the high efficiencies cannot be transferred from a punching to a milling process due to the changed melt flow in the different machining processes [17]. The nature of the GHz-burst machining is therefore still not clear. Assuming an increase of nonlinear effects in dielectric materials, investigations of the behavior of ceramics, glasses and crystals when machined with GHz-bursts are of interest. As an experimental approach a comparison of ablation rates achieved with GHz-bursts and single pulses for the machining of squares for some metals as well as for dielectric material are given in this work.

2. Experimental Set-Up

A PHAROS PH1-20 laser source emitting 230 fs pulses at a wavelength of 1028 nm with repetition rates between 1 kHz and 1 MHz was used. The system offered a bi – burst mode, i.e. the combination of bursts with 5.4 GHz (180 ps intra-burst time interval) and 65 MHz (15.4 ns intra-burst time interval). The maximum number of pulses per burst was limited to 25 and 8 for the GHz and the MHz burst, respectively. The energy of the single pulses in the burst, in GHz–case, was monitored with an ultrafast photodiode and a high bandwidth oscilloscope. As for stable operation the last pulse of the burst train had to cover the remaining part of the energy stored in the amplifier, an operation with identical energy per pulse in the burst was not possible. Fig. 1 shows the oscilloscope signals of the shapes set for 2, 3, 4, 8, 6 and 25 pulse GHz-bursts.

The laser was operated at its maximum power of about 20 W, which was then adjusted by turning a half-wave plate in front of a thin film polarizer. A set-up containing a telescope, to enlarge and collimate the beam and an excelliSCAN 14 galvo scanner with a $f=160 \text{ mm}$ f–theta objective was used. The corresponding spot size and beam quality factor amounted $w_0 = 16.2 \mu\text{m}$ with $M^2 = 1.35$. The scanner was fully synchronized [18] to the laser system.

The specific removal rate γ_{spec} i.e. the removed volume per energy unit was deduced for the number of pulses per burst $n_b = 1, 2, 3, 4, 8, 16$ and 25. Squares with a side length of $s = 1.6 \text{ mm}$ were machined into copper DHP, brass, steel 1.4301, silicon, zirconium oxide (ZrO_2), soda-lime glass and sapphire with a repetition rate of $f_{rep} = 100 \text{ kHz}$. For defined and reproducible starting conditions, the surface of the metal targets was lapped whereas the silicon target was a (100) single side polished p – type wafer of $650 \mu\text{m}$ thickness and having a surface resistance of $\rho = 1 - 100 \Omega\text{cm}$.

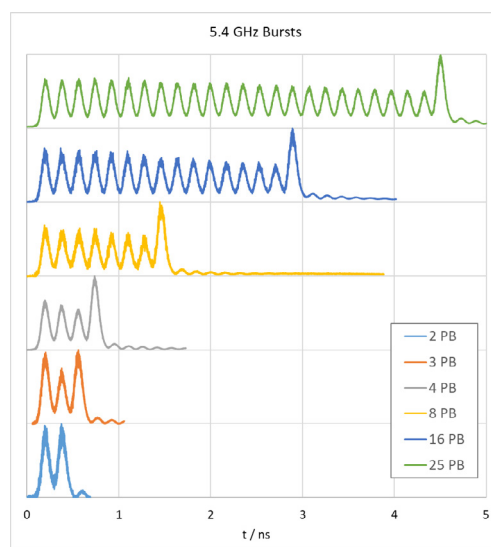


Fig. 1. Oscilloscope signals for 2, 3, 4, 8, 16 and 25 pulses per burst.

The average power P_{av} was increased, so the fluence reaches values from below the threshold to several J/cm^2 . In case of higher number of pulses per burst the applicable fluence was limited by the maximum average power of the system. The spot to spot distances in scan and cross-scan direction were set to $p_x = p_y = 8 \mu\text{m}$. The number of repetitions n_r was chosen accordingly to obtain a constant number of individual pulses per area i.e. $n_b \cdot n_r$ amounted 192 for steel, 96 for copper, brass and silicon respectively 48 for ZrO_2 , soda-lime glass and sapphire. Only for the 25 pulse burst this condition could not be fulfilled and the corresponding numbers amounted 200, 100 and 50. After cleaning in an ultrasonic bath the depth d of the squares and the surface roughness s_a were measured with an interferometric white – light microscope smartWLI from GBS. The specific removal rate was then deduced by

$$\gamma_{spec} = \frac{p_x \cdot p_y \cdot d \cdot f_{rep}}{n_b \cdot n_r \cdot P_{av}} \quad (1)$$

To verify the hypothesis of ablation cooling additional calorimetric experiments [7,13] were performed to deduce the energy remaining in the material for copper. For this special cooling effect, most of the heat is assumed to be carried away by ablation, before it diffuses into the material [14]. This should lead to a reduced residual heat η_{res} when the material is machined with GHz-bursts. In general, the specific removal rate and many other measures will be presented as a function of the mean peak fluence of a single pulse in the burst which is given by:

$$\phi_0 = \frac{2 \cdot P_{av}}{f_{rep} \cdot \pi \cdot w_0^2 \cdot n_b} \quad (2)$$

3. Experimental Results

3.1. Metals

All metals show a similar behavior, namely a strong drop in the specific removal rate for an increasing number of pulses per burst as shown for copper in Fig. 2. The maximum specific removal rate drops from about $3.1 \mu\text{m}^3/\mu\text{J}$ for single pulses down to about $0.25 \mu\text{m}^3/\mu\text{J}$ for the 16 pulse burst which is a drop of more than 90%. The corresponding surface roughness values as a function of the specific removal rate are shown in Fig. 3. For a 1 pulse burst the surface roughness amounts $s_a = 1.15 \mu\text{m}$ at the optimum point, whereas this value drops down to 200–260 nm for the 2, 3 and 4 pulse burst. But comparing the s_a values at identical specific removal rates reveals that even lower values are obtained with the 1 pulse burst i.e. the GHz burst mode has also no advantage concerning the surface roughness.

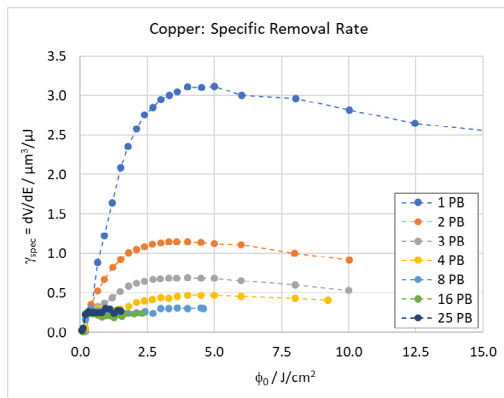


Fig. 2. Specific removal rate as a function of the sub – pulse mean peak fluence for the squares machined into copper with GHz – bursts.

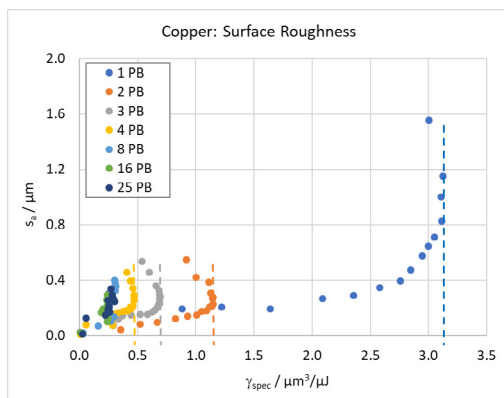


Fig. 3. Surface roughness dependent on the achieved specific removal rate

Steel and brass show similar behavior [19] and are therefore not discussed in detail here. The obtained maximum removal rates as well as the corresponding surface roughness values are summarized in Tab. 1. For all metals the maximum drop in the specific removal rate is tremendous and exceeds 90%.

Table 1: Maximum specific removal rates and surface roughness values as a function of the number of pulses per burst for all investigated metals.

Cu / #	1	2	3	4	8	16	25
$\gamma_{\max} / \mu\text{m}^3/\mu\text{J}$	3.12	1.15	0.69	0.47	0.31	0.24	0.3
$s_a / \mu\text{m}$	1.15	0.23	0.20	0.26	0.35	0.12	0.25
Brass / #	1	2	3	4	8	16	25
$\gamma_{\max} / \mu\text{m}^3/\mu\text{J}$	4.25	1.66	0.99	0.63	0.35	0.36	0.49
$s_a / \mu\text{m}$	0.47	0.24	0.29	0.27	0.42	0.14	0.17
Steel 1.4301 / #	1	2	3	4	8	16	25
$\gamma_{\max} / \mu\text{m}^3/\mu\text{J}$	4.87	0.85	0.50	0.48	0.31	0.33	0.39
$s_a / \mu\text{m}$	0.27	0.13	0.12	0.12	0.23	0.25	0.25

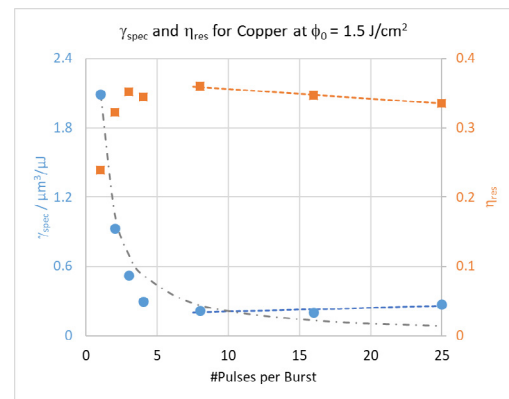


Fig. 4. Specific removal rate (blue circles) and residual heat (orange squares) as a function of the number of pulses per burst for copper at a mean peak fluence of 1.5 J/cm^2 . Complete shielding is represented by the black dash-dotted line.

For all investigated mean peak fluences the residual heat in copper increases from about 25% for the 1 pulse burst to above 30% for higher numbers of pulses per burst [19] illustrating that no ablation cooling effect is taking place or that it is at least not more pronounced compared to other situations. Fig. 4 shows the specific removal rate γ_{spec} and the corresponding residual heat η_{res} for a mean peak fluence of about 1.5 J/cm^2 (the maximum value for 25 pulse burst). The strong drop in the specific removal rate is expected to be caused by shielding effects and re-deposition of material [6,10]. Assuming a complete shielding of the 2 and all consecutive pulses in the burst with identical absorptance of the surface, would lead to specific removal rates, indicated by the black dash-dotted line in Fig. 4. If the measured value is above this line at least one of the subsequent pulses contributes to the material removal process. In contrast, if the measured value is lower, the subsequent pulses even hinders the material removal process of the first one i.e. they re-deposit material [12,13]. It can clearly be seen that this re-deposition occurs up to 8 pulses per bursts and from about 10 pulses on the subsequent pulses start to contribute to the ablation process again. Exactly from this point on the residual heat starts to slightly decrease i.e. the re-deposited material is expected to be responsible for the high increase of the residual heat. If for copper the removed material is assumed to be fully vaporized, a completely molten state at 1358 K as starting point, a vaporization temperature of 2870 K , a specific heat capacity of 385 J/kg/K and a specific

vaporization enthalpy of 4'730 kJ/kg the demanded energy per unit volume for this process would amount $0.0473 \mu\text{J}/\mu\text{m}^3$. Ellipsometry showed a reflectivity of $R_s = 0.966$ for a polished copper surface and $R_l = 0.94$ a surface slightly above the melting temperature [20]. With calorimetric experiments a reflectivity of a machined surface of about $R_{\text{eff},s} = 0.55$ was measured for the 25 pulse burst. From this the reflectivity of the molten surface can be estimated by $R_{\text{eff},l} = R_{\text{eff},s} \cdot R_l / R_s = 0.438$. But for a Gaussian beam and the Lambert-Beers law for absorption, a maximum part of $2/e^2 = 0.27$ of the energy can really be transferred to removed material [3]. Taking this into account a maximum volume of $3.21 \mu\text{m}^3$ per μJ of incoming energy can be evaporated. Specific removal rates of copper above this value can therefore only be achieved if a relevant part of the removed materials is only melted and not vaporized i.e. melt ejection is responsible for the higher rates. The reported values of $7.6 \mu\text{m}^3/\mu\text{J}$ [14] and $11.5 \mu\text{m}^3/\mu\text{J}$ [16] are definitively above the value of the calculated threshold of $3.21 \mu\text{m}^3/\mu\text{J}$ and therefore a high amount of melt ejection and not an ablation cooling effect is assumed to be responsible for this reported high removal rates.

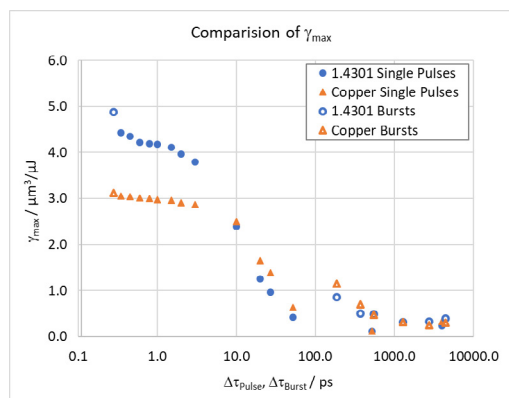


Fig. 5. Maximum specific removal rates for copper (triangles) and steel 1.4301 (circles) for one pulse bursts (filled) and bursts with 2-25 pulses per burst (white) as a function of the pulse and burst duration, respectively.

If the obtained maximum specific removal rates for copper and steel 1.4301 of the presented burst experiments are compared with the equivalent values for single pulses (1 pulse bursts) of different pulse duration, an identical trend is observed as illustrated in Fig. 5 thus for the presented milling application, the GHz bursts follow exactly the same trend as single pulses of corresponding pulse duration. This is also the case for punching applications in copper, aluminum and steel with 200 pulses of a 1.76 GHz burst compared with a single pulse of 100 ns pulse duration [16].

3.2. Silicon

For silicon the maximum specific removal rate drops less pronounced up to 8 pulses per burst and then increases from about $1.0 \mu\text{m}^3/\mu\text{J}$ to $1.6 \mu\text{m}^3/\mu\text{J}$ for the 25 pulse burst.

Table 2: Maximum specific removal rates and surface roughness for silicon.

Si / #	1	2	3	4	8	16	25
$\gamma_{\text{max}} / \mu\text{m}^3/\mu\text{J}$	4.46	1.68	1.17	1.12	1.01	1.09	1.60

$s_a / \mu\text{m}$	3.86	0.24	0.38	0.47	0.56	0.57	0.71
---------------------	------	------	------	------	------	------	------

The surface roughness is very high due to cavity formation for single pulses, then strongly decreases for a 2 pulse burst and increases up to the 25 pulse burst. All values are summarized in Tab. 2.

3.3. Zirconium Oxide, ZrO₂

The results for the specific removal rate of ZrO₂ are shown in Fig. 6 and its maximum values summarized in Tab. 3. Its maximum value increases by about 10% when the number of pulses per burst is raised from 1 to 4 and the decreases to 85% for the 25 pulse burst, variations which are much lower than for the investigated metals. The optimum fluence, where the maximum specific removal rates are obtained, continuously decrease from $5.60 \text{ J}/\text{cm}^2$ for a 1 pulse burst down to $0.65 \text{ J}/\text{cm}^2$ for a 25 pulse burst. The surface roughness values at these optimum points are given in Tab. 3. The lowest roughness is obtained for the 3 and 4 pulse burst, where the highest specific removal rates are obtained.

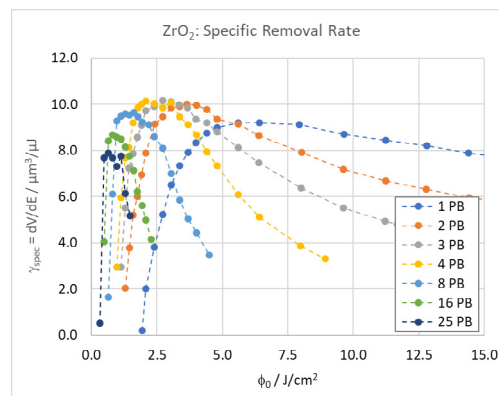


Fig. 6. Specific removal rate as a function of the sub – pulse mean peak fluence for the squares machined into ZrO₂ with GHz–bursts.

Table 3: Maximum specific removal rates and surface roughness for ZrO₂.

ZrO ₂ / #	1	2	3	4	8	16	25
$\gamma_{\text{max}} / \mu\text{m}^3/\mu\text{J}$	9.20	10.0	10.2	10.1	9.63	8.68	7.88
$s_a / \mu\text{m}$	1.21	0.76	0.69	0.66	0.72	0.77	0.81

3.4. Sapphire and Soda-lime Glass

Sapphire and soda-lime glass both show a tremendous increase of the specific removal rates for increasing pulses in the burst. As indicated in Fig. 7 for both materials this increase follows nearly a linear trend for the investigated number of pulses per burst. Furthermore, a massive reduction of the optimal fluence and the threshold fluence is observed.

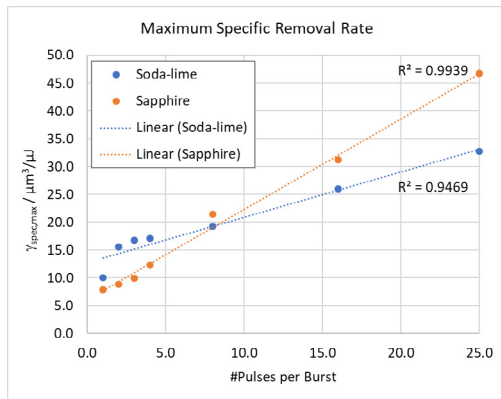


Fig. 7. Maximal specific removal rates for sapphire and soda-lime glass as a function of the number of pulses per GHz – bursts.

For sapphire a maximum specific removal rate of $46.7 \mu\text{m}^3/\mu\text{J}$ is achieved for the 25 pulse burst. This value exceeds the maximum obtained for single pulses by nearly a factor of 6 and is reached at an optimal fluence of $0.5 \text{ J}/\text{cm}^2$. Higher fluences lead to a drastic reduction of the specific removal rate whereas for lower ones no direct ablation, but the induction of cracks is observed. Likewise, high maximum specific removal rates are reached with 16 and 8 pulses per bursts and a similar behavior is observed as shown in Fig. 8.

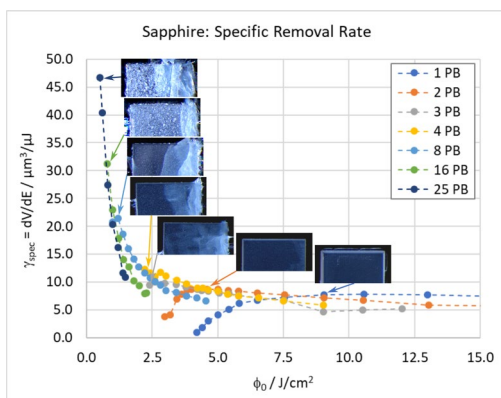


Fig. 8. Specific removal rate as a function of the sub – pulse mean peak fluence for the squares machined into Sapphire with GHz – bursts. Microscopy images indicate the quality obtained at the particular maximum specific removal rates.

By analyzing the surface roughness and the visual inspection, a reduction of the quality is observed for increasing number of pulses per burst. Especially for squares corresponding to the maximum specific removal rates for 8 to 25 pulses per burst higher s_a values are measured as listed in Tab. 4. Furthermore, splitting and cracking of the surface and border is observed for these parameters as shown in the microscopy images in Fig 8. Therefore, it is assumed, that machining in this regime, induces tension and stress which lead to spallation of relatively big material parts.

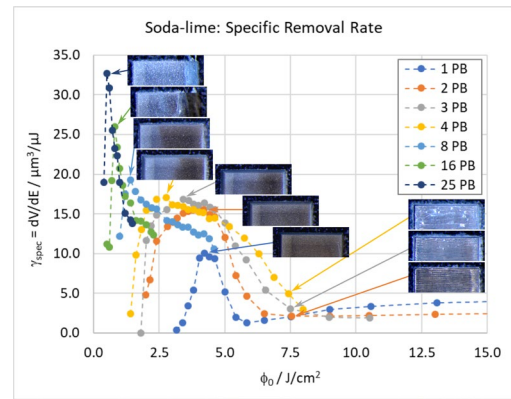


Fig. 9. Specific removal rate as a function of the sub – pulse mean peak fluence for the squares machined into soda-lime glass with GHz – bursts. Microscopy images indicate the quality obtained at particular specific removal rates.

For soda-lime glass a maximum specific removal rate of $32.7 \mu\text{m}^3/\mu\text{J}$ is achieved at an optimal fluence of $0.5 \text{ J}/\text{cm}^2$ for the 25 pulse burst, as illustrated in Fig 9. This rate exceeds the value for single pulse by a factor of more than 3.2. A similar behavior with a strong decrease is observed for 25, 16 and 8 pulses per bursts as described for sapphire. However, cracks in the surface and border are much less pronounced and appear mainly for 25 and 16 pulses per burst. Furthermore, no significant increase of the surface roughness is indicated.

Table 4: Maximum specific removal rates and surface roughness values as a function of the number of pulses per burst for sapphire and soda-lime glass.

Sapphire / #	1	2	3	4	8	16	25
$\gamma_{\text{max}} / \mu\text{m}^3/\mu\text{J}$	7.86	8.80	9.95	12.3	21.5	31.3	46.7
$s_a / \mu\text{m}$	0.77	0.52	0.75	1.02	1.87	3.85	6.52
Soda-lime / #	1	2	3	4	8	16	25
$\gamma_{\text{max}} / \mu\text{m}^3/\mu\text{J}$	10.1	15.6	16.8	17.1	19.3	26.0	32.7
$s_a / \mu\text{m}$	1.15	1.48	2.11	1.54	1.46	1.80	2.77

As illustrated on the right-hand side of Fig. 9 soda-lime glass shows a special behavior for fluences above the optimum for 1 to 4 pulses per burst. Around the drop of the specific removal rate, flat surfaces with reduced scattering properties, but horizontal cracks are obtained. A similar behavior was already reported [21] and the occurrence of melting during the process was demonstrated by SEM images.

Conclusion

Copper, brass, steel, silicon, ZrO_2 , soda-lime glass and sapphire were machined in a milling application with 5.4 GHz bursts and up 25 pulses per burst. For the metals and silicon, the previously reported very high removal rates for punching applications could definitely not be confirmed, on the contrary, the specific removal rate tremendously dropped down by 90% or more for the metals and 60% for silicon for a 25 pulse burst, as illustrated in Fig. 10. The experiments disproved the existence of an enhanced ablation cooling effect. The fact that for both, milling and punching applications, the removal rates equals the ones of single pulses with

corresponding pulse durations further indicates, that the reported high removal rates for punching applications are caused by increased melt ejection.

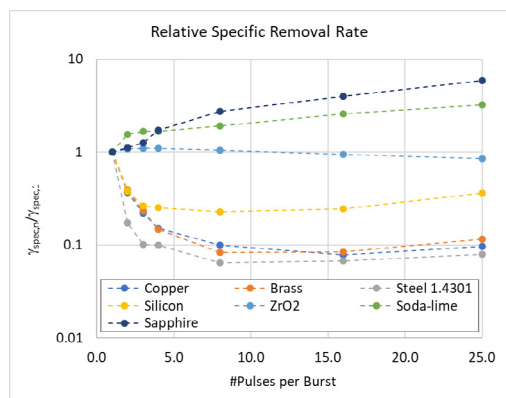


Fig. 10. Relative specific removal rate in logarithmic scale as a function of the number of pulses per burst for all investigated materials.

The situation differs for ZrO₂, soda-lime glass and sapphire. For ZrO₂ the specific removal rate was only minor influenced by the number of pulses per burst and the lowest surface roughness was achieved at the bursts with the highest specific removal rate. Thus, GHz bursts with 3 to 8 pulses could ideally be suited to machine this ceramic, but experiments with standard MHz bursts should be performed first to foster this assumption.

Soda-lime glass and sapphire show both a significant increase of the specific removal rate when they are machined with GHz bursts (see Fig. 10). For both material the optimum fluence going with the highest specific removal rate drops with the number of pulses per burst. The two glasses differ concerning the surface roughness. Whereas for sapphire these values at the optimum fluence almost linearly increase with the number of pulses per burst, no significant difference was measured for soda-lime glass. Further experiments with single ns pulses of corresponding duration and conventional MHz bursts with equivalent number of pulses per burst are demanded to gain a clearer picture of GHz ablation. The influence of nonlinear absorption is assumed to be significant in GHz burst processes for glasses and other transparent materials.

Acknowledgements

The authors wish to thank Patrick Neuenschwander for his help with the WLI microscopy.

References

[1] Furmanski J, Rubenckick AM, Shirk MD, Stuart BC. Deterministic processing of alumina with ultrashort pulses. *Journal of Appl. Phys* 2007;102:073112.

[2] Raciukaitis G, Brikas M, Gecys P, Voisiat B, Gedvilas M. Use of high repetition rate and high power lasers in microfabrication: How to keep the efficiency high?. *JLMN J. of Laser Micro/Nanoengineering* 2009;4:186.

[3] Neuenschwander B, Jaeggi B, Schmid M, Hennig G. Surface Structuring with ultra-short laser pulses: Basics, limitations and needs for high throughput. *Phys. Procedia* 2014;56:1047-1058.

[4] Jaeggi B, Remund SM, Streubel R, Goekce B, Barcikowski S, Neuenschwander B. Laser Micromachining of Metals with Ultra-Short Pulses: Factors Limiting the Scale-Up Process. *J. of Laser Micro/Nanoengineering* 2017;12:267-273.

[5] Schille J, Schneider L, Streek A, Kloetzer S, Loeschner U. High-throughput machining using a high-average power ultrashort pulse laser and high-speed polygon scanner. *Optical Engineering* 2016;55:096109.

[6] Koenig J, Nolte S, Tuennermann A. Plasma evolution during metal ablation with ultrashort pulses," *Optics Express* 2005;13:10597-10607.

[7] Bauer F, Michalowski A, Kiedrowski T, Nolte S. Heat accumulation in ultra-short pulsed scanning laser ablation of metals. *Optics Express* 2015;23:1035-1043.

[8] Knappe R, Haloui H, Seifert A, Weis A, Nebel A. Scaling ablation rates for picosecond lasers using burst micromachining. *Proc. of SPIE* 2010;7585:75850H.

[9] Neuenschwander B, Kramer T, Lauer B, Jaeggi B. Burst mode with ps- and fs-pulses: Influence on the removal rate, surface quality and heat accumulation. *Proc. of SPIE* 2015;9350:93500U.

[10] Jaeggi B, Remund SM, Zhang Y, Kramer T, Neuenschwander B. Optimizing the Specific Removal Rate with the Burst Mode Under Varying Conditions. *JLMN J. of Laser Micro/Nanoengineering* 2017;12:258-266.

[11] Bornschelegel B, Finger J. In-Situ Analysis of Ultrashort Pulsed Laser Ablation with Pulse Bursts. *JLMN J. of Laser Micro/Nanoengineering* 2019;14:88-94.

[12] Foerster DJ, Faas S, Groeninger S, Bauer F, Michalowski A, Weber R, Graf T. Shielding effect and re-deposition of material during processing of metals with burts of ultra-short laser pulses. *Appl. Surf. Sci* 2018;440:926-931.

[13] Neuenschwander B, Jaeggi B, Foerster DJ, Kramer T, Remund SM. Influence of the burst mode onto the specific removal rate for metals and semiconductors. *Journal of Laser Applications* 2019;31:022203.

[14] Kerse C, Kalaycioglu H, Elahi P, Cetin B, Kesim DK, Akcaalan Ö, Yavas S, Asik MD, Öktem B, Hoogland H, Holzwarth R, Ömer–Ilday F. Ablation-cooled material removal with ultrafast bursts of pulses. *Nature* 2016;532:84-89.

[15] Mischik K, Bonais G, Qiao J, Lopez J, Audouard E, Mottay E, Hönninger C, Manek-Hönninger I. High-efficiency femtosecond ablation of silicon with GHz repetition rate laser source. *Opt. Lett.* 2019;44:2193-2196.

[16] Bonamis G, Mischik K, Audouard E, Hönninger C, Mottay E, Lopez J, Manek-Hönninger I. High efficiency femtosecond laser ablation with gigahertz level bursts. *J. Laser Appl.* 2019;31:022205.

[17] Matsumoto H, Zhibin L, Kleinert J. Ultrafast laser ablation of copper with GHz-bursts," *Proc. of SPIE* 2018;10519:1051902.

[18] Jaeggi B, Neuenschwander B, Zimmermann M, Zecherle M, Boeckler EW. Time-optimized laser micromachining by using a new high dynamic and high precision galvo scanner. *Proc of SPIE* 2016;9735:973513.

[19] Hirsiger T, Gafner M, Remund SM, Chaja MV, Urniezius A, Butkus S, Neuenschwander B. Machining metals and silicon with GHz bursts: Surprising tremendous reduction of the specific removal rate for surface texturing applications. *Proc. of SPIE* 2013;11267:112670T.

[20] Schmid M, Zehnder S, Schwaller P, Neuenschwander B, Zuercher J, Hunziker U. Measuring the complex refractive index of metals in the solid and the liquid state and its influence on the laser machining. *Proc. of SPIE* 2013;8607:86071I.

[21] Neuenschwander B, Jaeggi B, Schmid M. From ps to fs: Dependence of the Material Removal Rate and the Surface Quality on the Pulse Duration for Metals, Semiconductors and Oxides. *Proc. of ICALEO* 2012:ICA_12_M1004